Electronic Supplementary Information

Donor-acceptor liganded metal-organic framework showcases hydrogen-bonds enhanced sensing of N-heterocyclic explosives

Junjie Wang, Yao Cheng, Jie Zhou, Weihua Tang*

Table of Contents

1. Materials and characterization

All reagents and chemicals were purchased through commercial channels. 2,7-Dibromo-9-fluorenone, 4-(4,4,5,5-tetramethyl-1,3,2-dioxaborolan-2-yl)pyridine, [1,1'-biphenyl]-4,4'-dicarboxylic acid, 4-nitrotoluene, toluene, $Zn(NO_3)_2 \cdot 6H_2O$ were purchased from Shanghai Bidepharm Technology Co., Ltd. 3-Nitrophenol, 4-nitrophenol, $MgSO_4$ and K_2CO_3 were purchased from Shanghai Macklin Biochemical Co., Ltd. Ethyl alcohol, petroleum ether, ethyl acetate and dichloromethane were purchased from Shanghai Titan Technology Co., Ltd. N,N-dimethylformamide and $Pd(PPh_3)_4$ were purchased from Energy-chemical (Shanghai, China). Acetonitrile, 1,4-dinitrobenzene, nitrobenzene was purchased from Shanghai Aladdin Biochemical Technology Co., Ltd. 2-Nitro-2-(1H-1,2,4-triazol-5-yl)ethene-1,1-diamine (TriazFOX) and 2-nitro-2-(2H-tetrazol-5-yl)-1,1-ethenediamine (TetrazFOX) were provided by Tang's group.

Powder X-ray diffraction (PXRD) measurements were recorded from Bruker D8 Advance Diffractometer with Cu-Kα radiation and the data were collected within the 2θ in range of 5-40°. The morphologies of materials were observed by a FEI400FEG scanning electron microscopy (SEM). High-resolution transmission electron microscopy (TEM) was carried out on JEOL JEM-2100F electron microscope. NMR spectra were measured at on AVANCE III 500 MHz Digital NMR Spectrometer. Fourier transform infrared (FTIR) spectrometer (Nicolet IS-10, USA) is used to measure the transmittance spectra in the range of 4000–500 cm^{-1}. UV-visible absorption spectra were measured on an EV 200 instrument. Thermal analysis was performed using TGA/SDTA851E (Mettler Toledo) with a heating rate of 20°C min^{-1} in N_2 atmosphere. N_2 gas adsorption measurements on ZnMOF-1 were performed using Micromeritics 3-Flex. Fluorescence spectra were recorded on RF-6000 Spectro Fluorimeter.
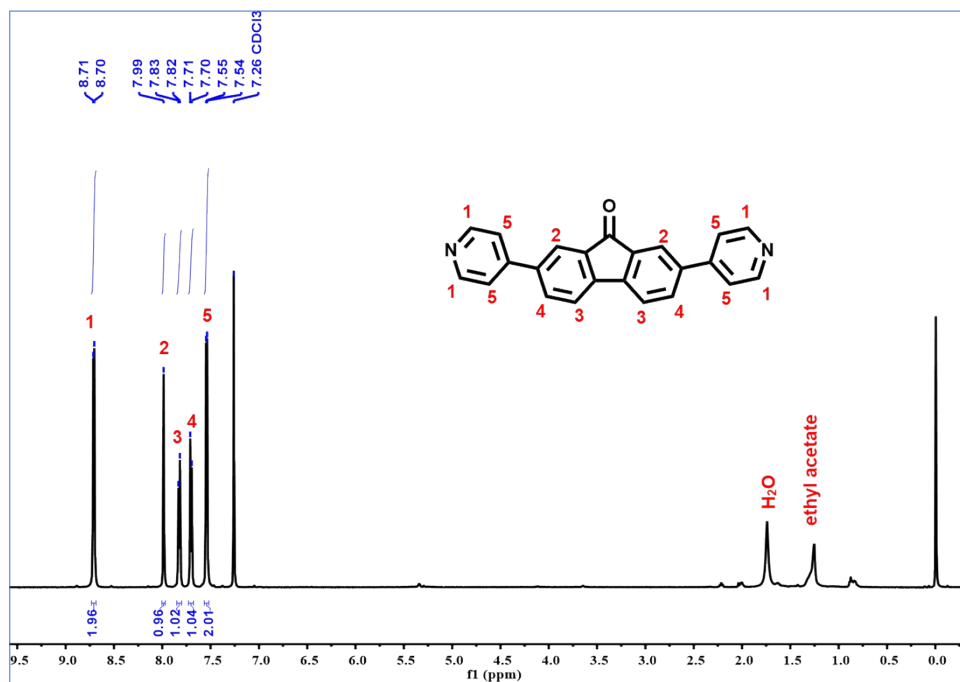
2. NMR and mass spectra
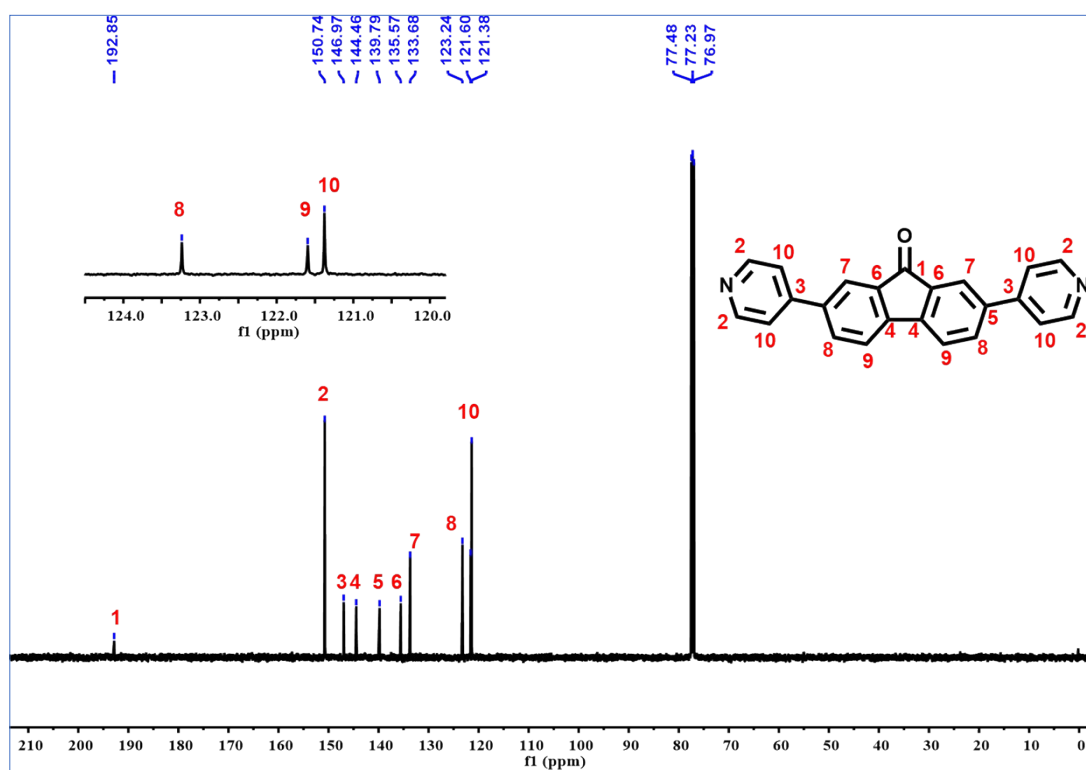
Figure S1. 500 MHz ^{1}H NMR spectrum of DPyF.

Figure S2. 500 MHz ^{13}C NMR spectrum of DPyF.
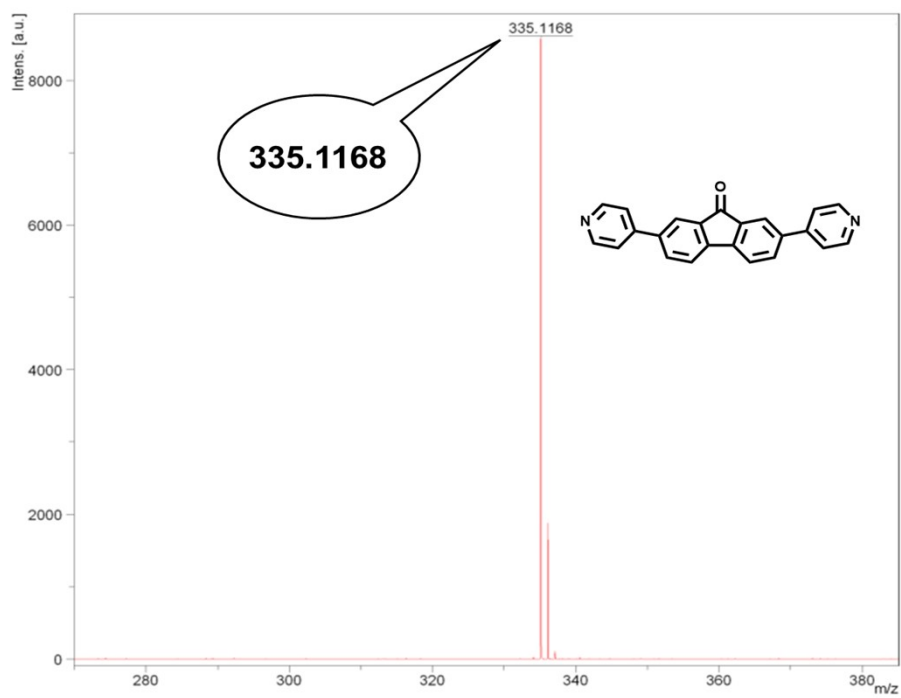
Figure S3. Mass Spectrum of DPyF.
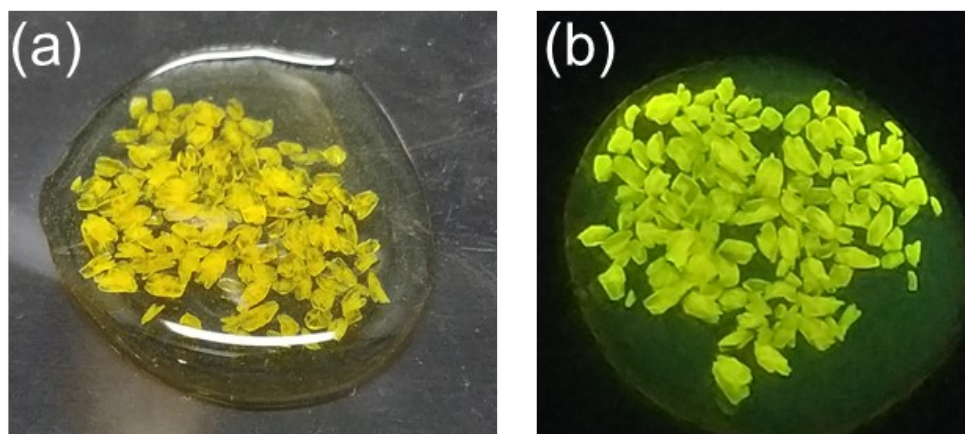
3. Morphology observation

Figure S4. The crystals structural of ZnMOF-1 at daylight (a) and 365 nm UV light (b).
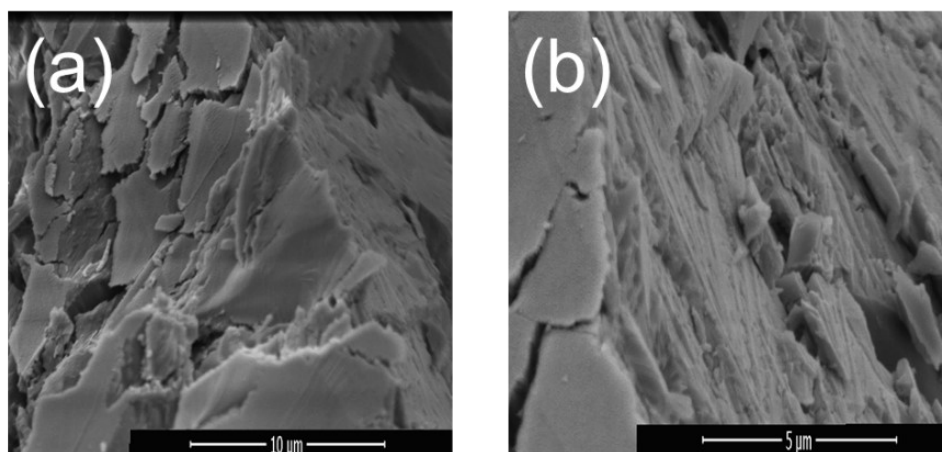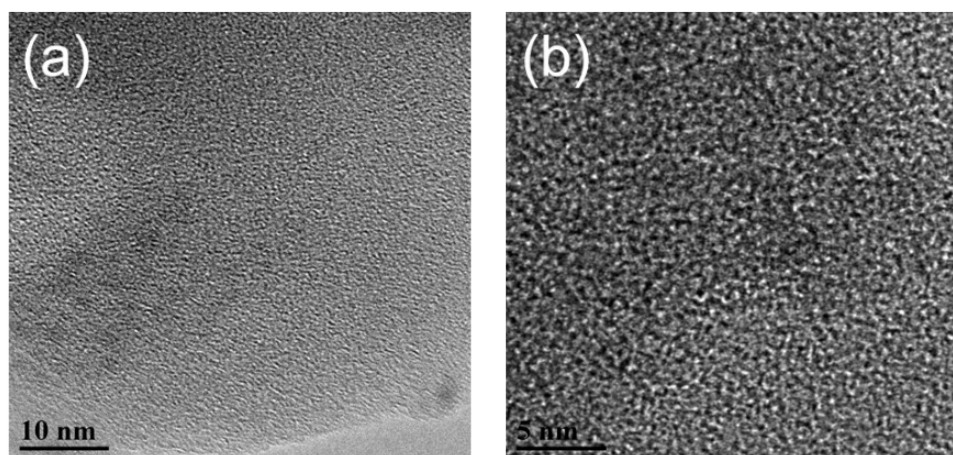

Figure S5. SEM image of ZnMOF-1

Figure S6. HRTEM image of ZnMOF-1.
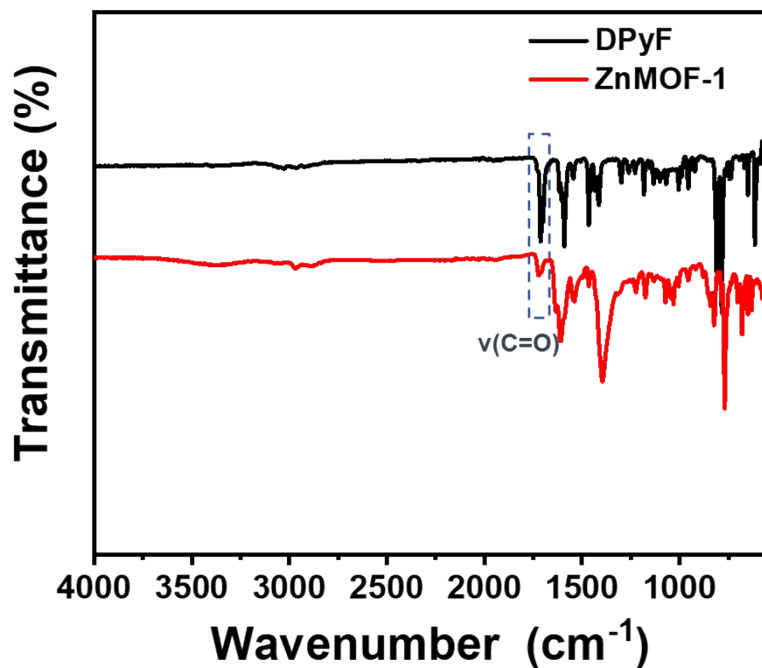
4. FT-IR spectra and TGA analysis

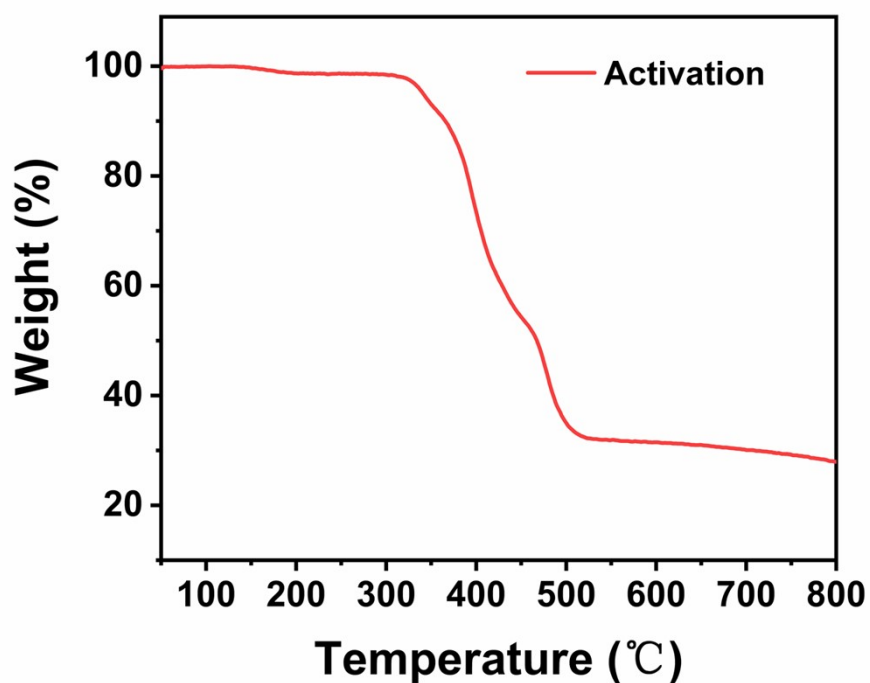**Figure S7.** FTIR spectra of ZnMOF-1 and DPyF.

Figure S8. Thermogravimetric Analysis curve for activated ZnMOF-1.

5. Single crystal XRD data

Table S1. Crystal data and structure refinement for ZnMOF-1.

Compound	ZnMOF-1	
Empirical formula	$C_{51}H_{30}N_2O_9Zn_2$	
Formula weight	945.51	
Temperature	296(2) K	
Wavelength	0.71073 Å	
Crystal system	Triclinic	
Space group	P1	
Unit cell dimensions	a = 15.147(3) Å	a= 106.792(6)°.
	b = 15.168(3) Å	b= 103.569(6)°.
	c = 22.006(5) Å	g = 101.715(6)°
Volume	4501.5(17) $Å^3$	
Z	3	
Density (calculated)	1.046 Mg/m^3	
Absorption coefficient	0.844 mm^{-1}	
F(000)	1446	
Crystal size	0.220 x 0.180 x 0.160 mm^3	
Theta range for data collection	2.045 to 24.999°.	
Index ranges	-18<=h<=18, -18<=k<=18, -25<=l<=26	
Reflections collected	51906	
Independent reflections	28717 [R(int) = 0.0538]	
Completeness to theta = 24.999°	98.5 %	
Absorption correction	Semi-empirical from equivalents	
Max. and min. transmission	0.7456 and 0.6043	
Refinement method	Full-matrix least-squares on F^2	
Data / restraints / parameters	28717 / 3003 / 1730	
Goodness-of-fit on F^2	1.045	
Final R indices [I>2sigma(I)]	R1 = 0.0575, wR2 = 0.1418	
R indices (all data)	R1 = 0.0887, wR2 = 0.1577	
Absolute structure parameter	0.504(15)	
Extinction coefficient	n/a	
Largest diff. peak and hole	0.995 and -0.597 $e.Å^{-3}$	

6. Structural modelling of MOF

Table S2. Hydrogen bonds for ZnMOF-1 [Å and °].

D-H...A	d(D-H)	d(H...A)	d(D...A)	<(DHA)
C(48)-H (48)...O(7)#1	0.93	2.50	3.083(12)	120.7
C(83)-H (83)...O(9)#2	0.93	2.50	3.269(13)	140.6
C(99)-H (99)...O(10)	0.93	2.60	3.281(13)	130.6
C(100)-H (100)...O(16)#3	0.93	2.60	3.065(12)	111.5
C(134)-H (134)...O(19)	0.93	2.42	3.147(13)	134.9

Symmetry transformations used to generate equivalent atoms:
#1 x-1,y+1,z+1   #2 x,y,z-1   #3 x,y,z+1
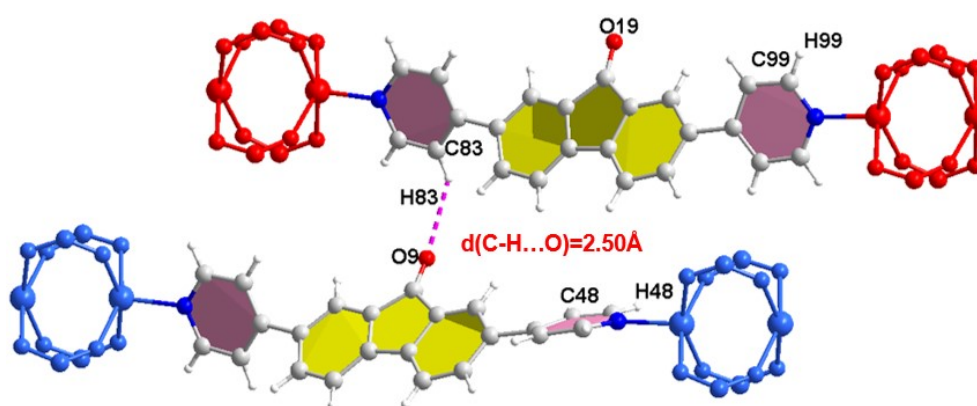
Figure S9. The hydrogen-bond linkages between the oxygen atom of the carbonyl functional group and the hydrogen atom of the of pyridine from the other frame.
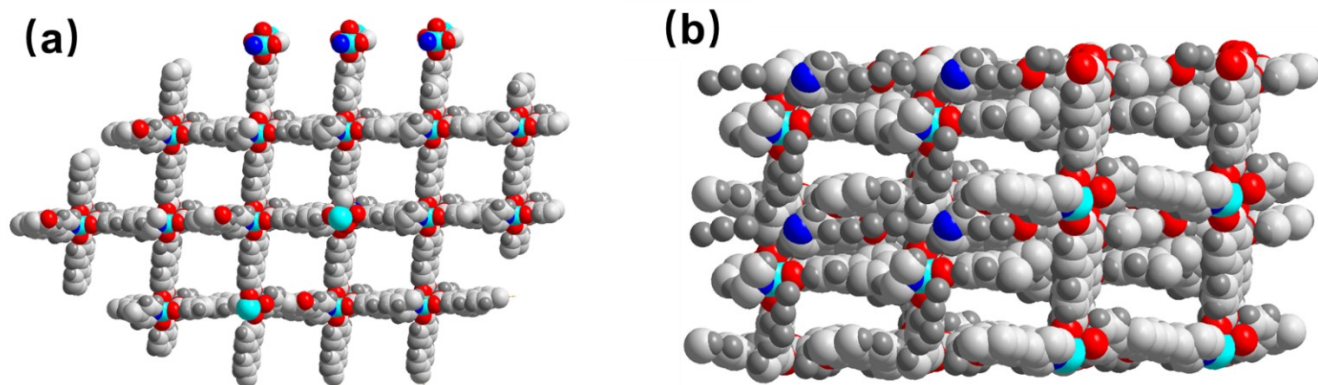

Figure S10. (a) Simplified framework structures of ZnMOF-1. (b) The structures were stacked in a three-fold interdigitated fashion to form three interpenetrating 3D frames.
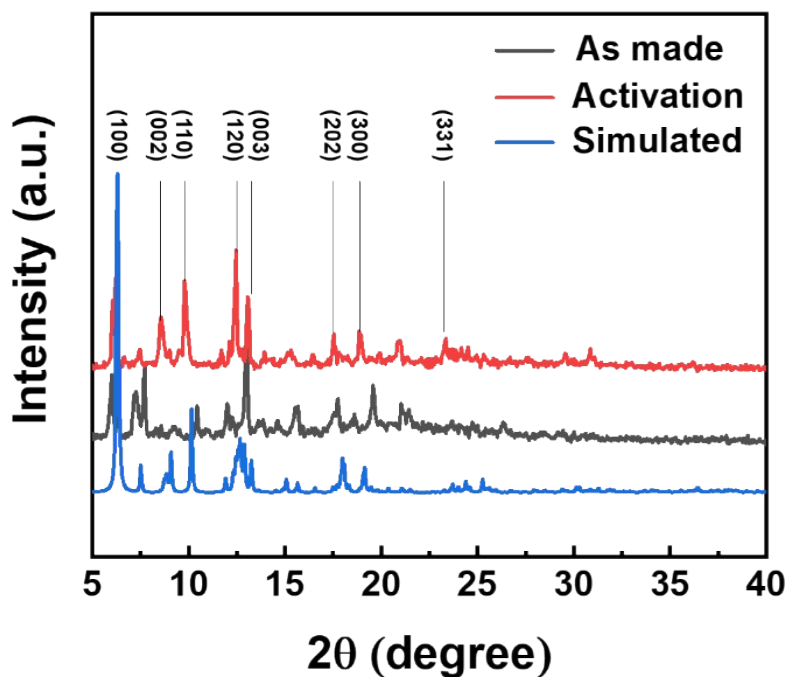
8

7. Powder XRD and BET analysis

Figure S11. Powder X-ray diffraction (PXRD) patterns of simulated (blue), as-made (black), and activation (red) ZnMOF-1
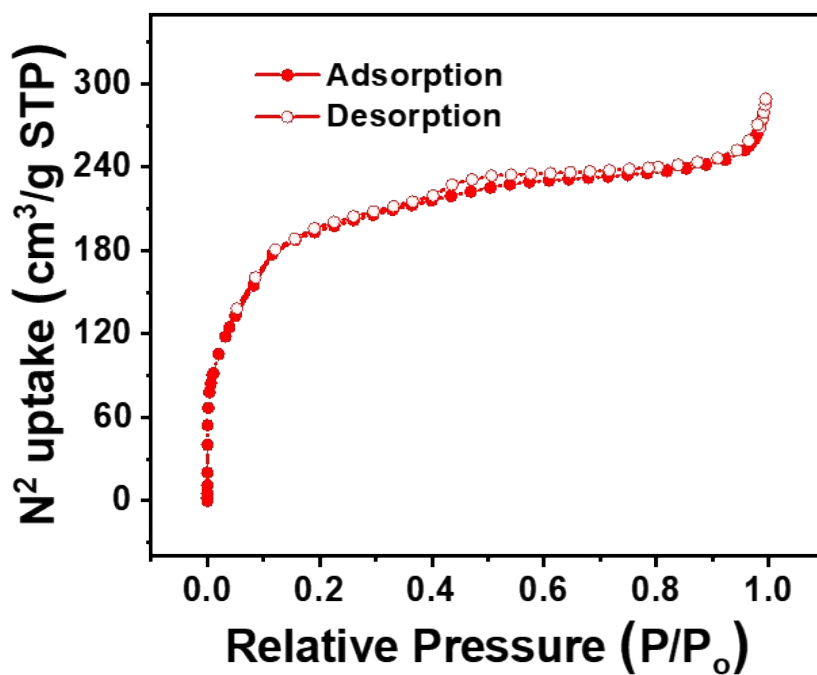

Figure S12. N_2 adsorption and desorption isotherms of degassed ZnMOF-1 at 77K.
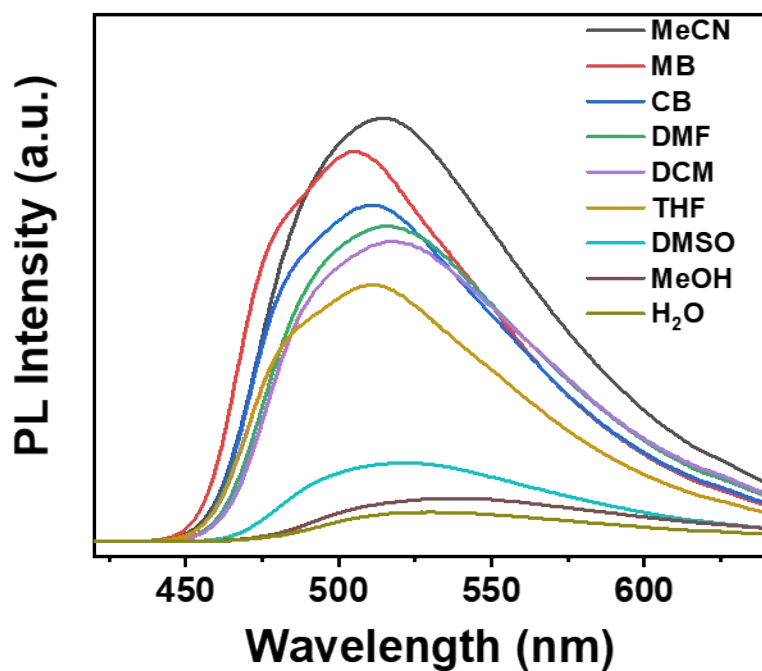
8. PL studies

Figure S13. Fluorescence intensities of ZnMOF-1 in different solvents (λ_{ex} = 328 nm).

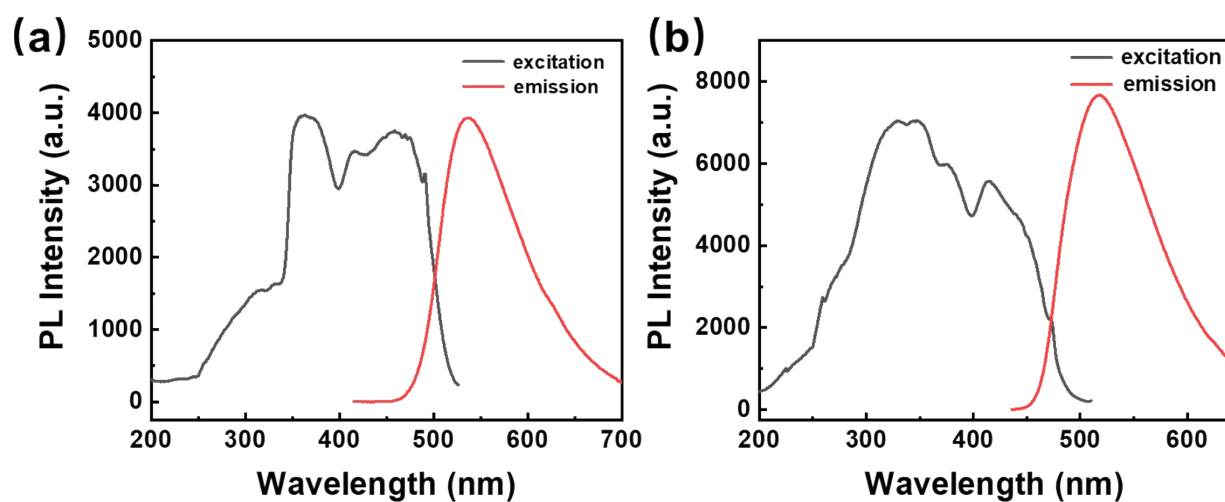**Figure S14.** The excitation and emission spectra of (a) DPyF ligand and (b) ZnMOF-1 in MeCN solutions

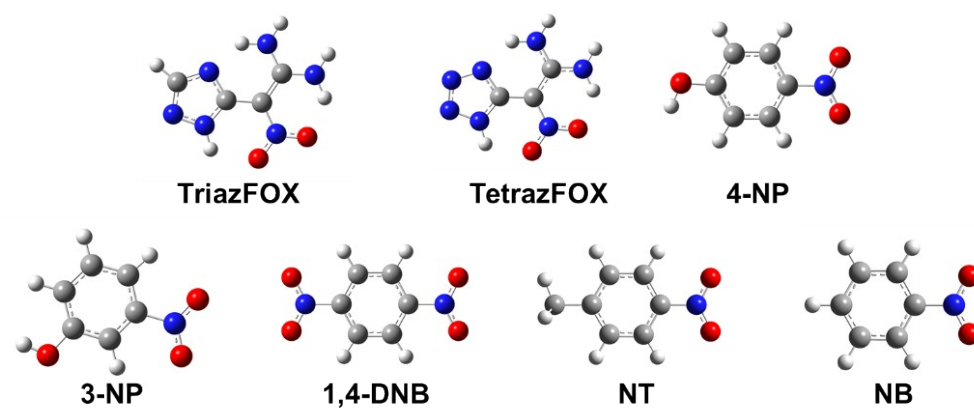## 9. Modelling of explosives

Figure S15. Molecular structures of the nitro-explosives.

Table S3 Molecular sizes of nitro-explosives（a, b, c are the length, width and height of the molecules）

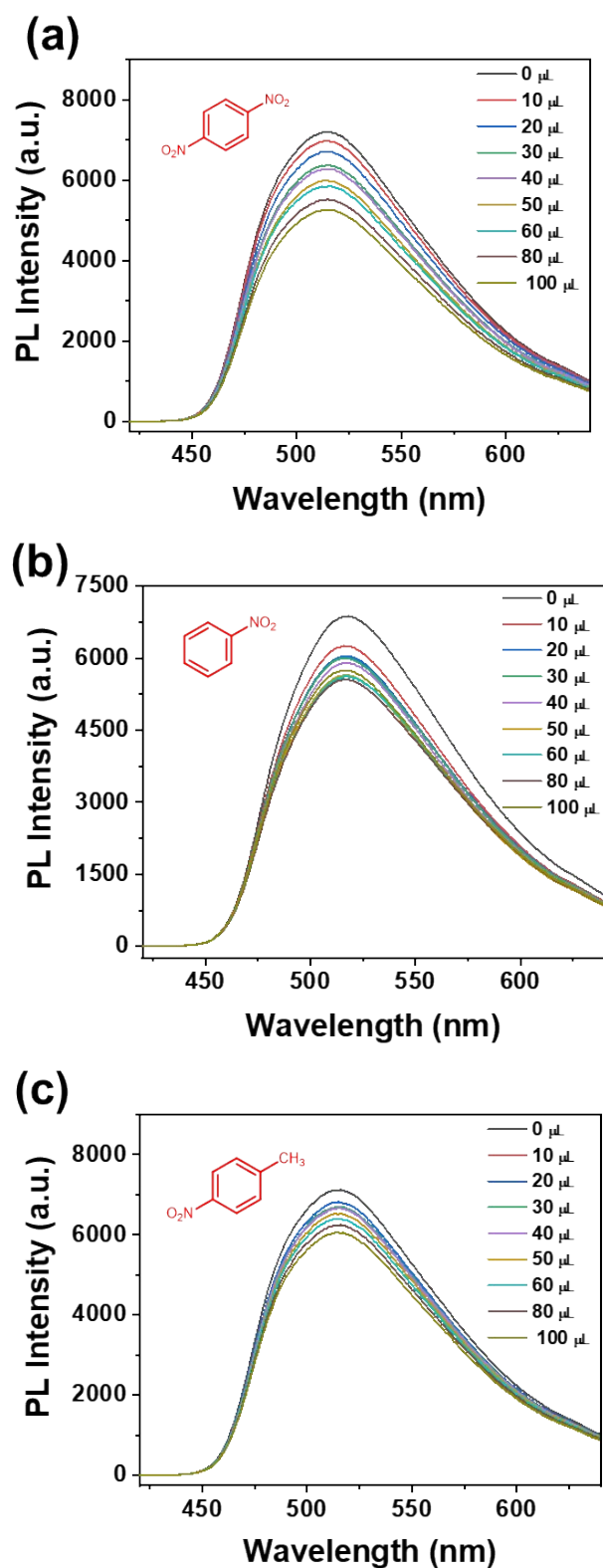| Dimension	TriazFOX	TetrazFOX	4-NP	3-NP	NT	NB	1,4-DNB
a (Å)	9.372	8.948	9.251	9.131	9.466	8.611	9.856
b (Å)	8.255	8.265	6.702	7.222	6.698	7.704	6.686
c (Å)	2.758	2. 752	3.040	2.722	4.162	3.040	3.040

10. Explosive detection with MOF

Figure S16. Quenching spectra for MOF solutions in MeCN with additions of 5 mM solutions of nitrobenzene compounds (a) 1,4-DNB, (b) NB and (c) NT.
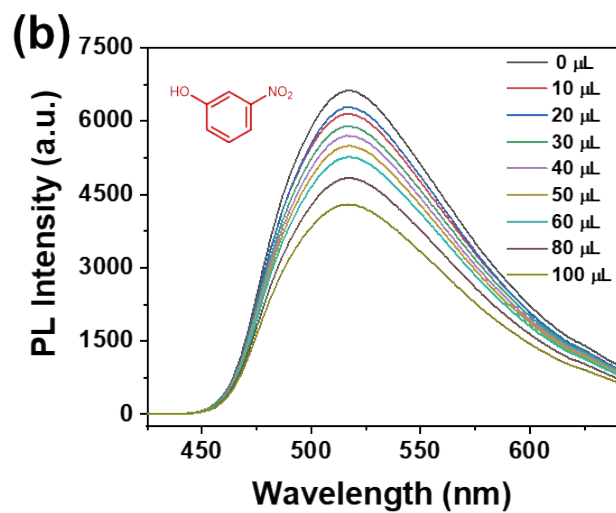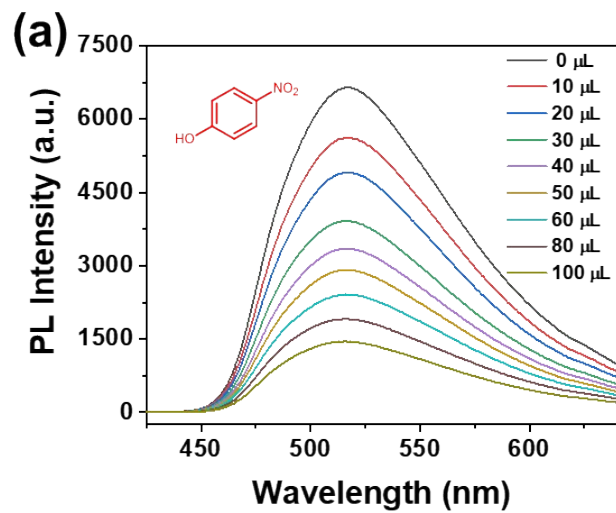
Figure S17. Quenching spectra for MOF solutions in MeCN with additions of 5 mM solutions of nitrophenol compounds (a) 4-NP and (b) 3-NP.
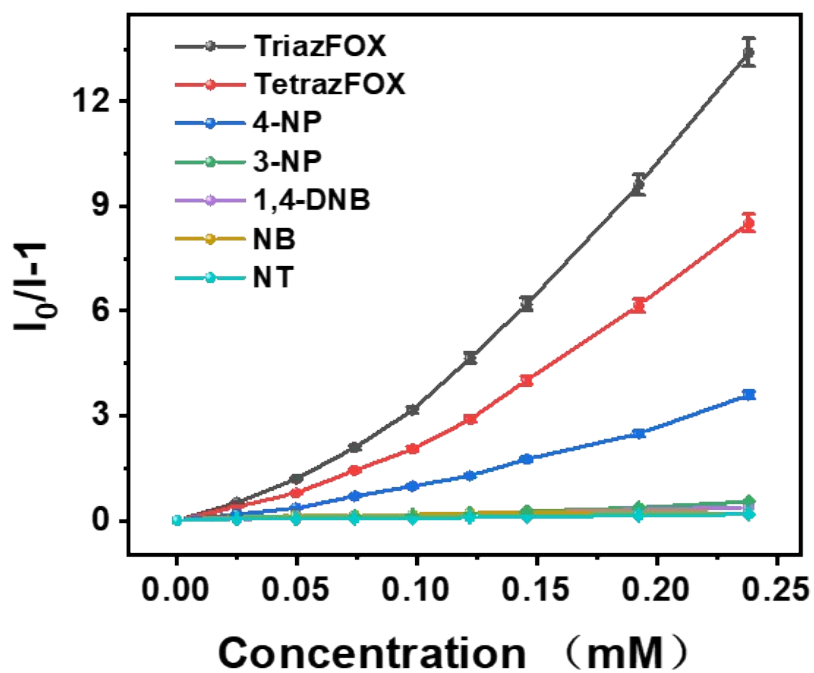
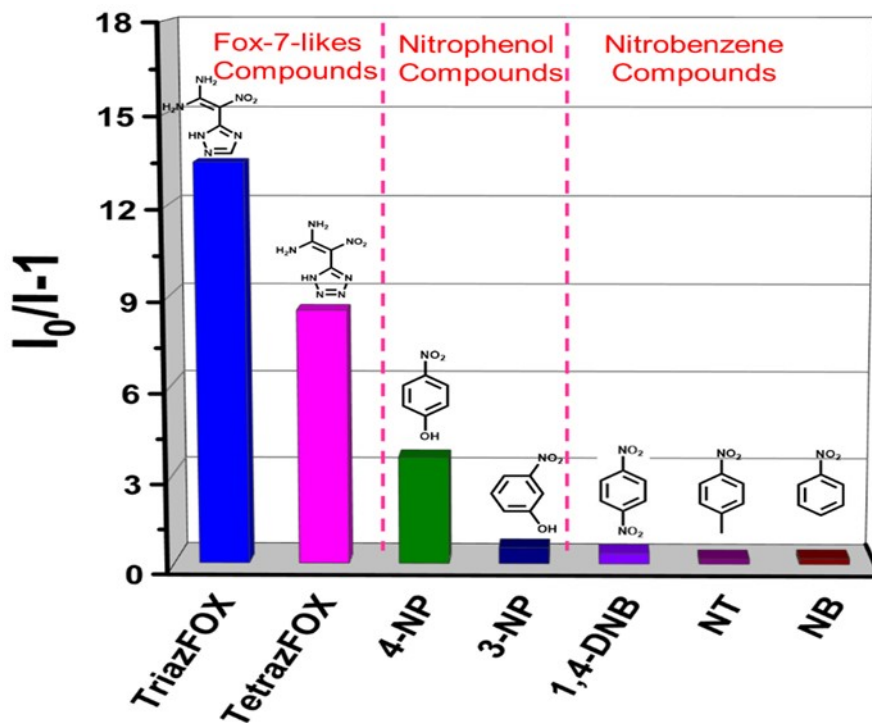**Figure S18.** Stern-Volmer plot of MOF by gradual addition of different explosives in MeCN solutions

Figure S19. Quenching efficiency [$(I_0/I-1)\times100\%$] obtained from different explosive for ZnMOF-1.

11. Modelling for the detection mechanism

(a)

Binding Energy= -0.67 eV

(b)

Binding Energy= -0.57 eV

(c)

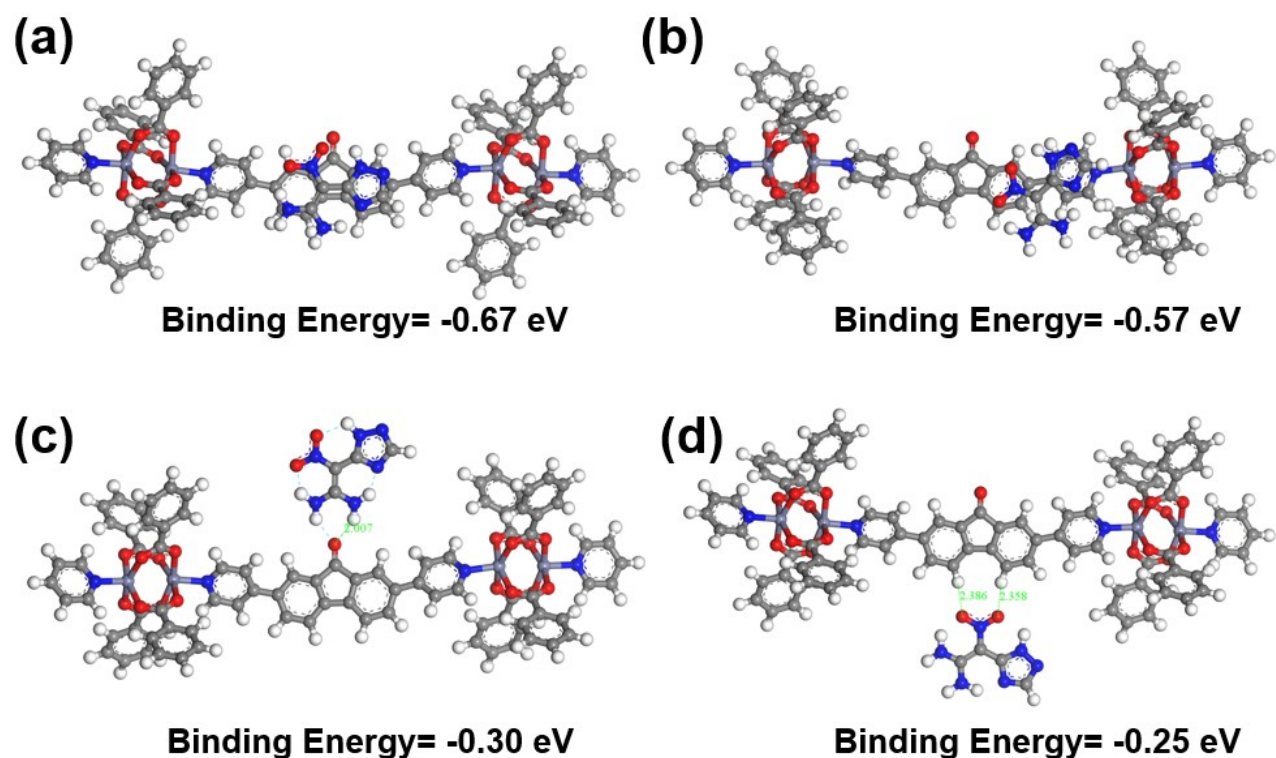Binding Energy= -0.30 eV

(d)

Binding Energy= -0.25 eV

Figure S20. Four models constructed between TriazFOX and ZnMOF-1 on the basis of: (a) π-π interaction within fluorenone core, (b) π-π interaction surrounding pyridine end. (c) dipole-dipole interaction and hydrogen bonding interaction within fluorenone core. (d) dipole-dipole interaction within fluorenone core.
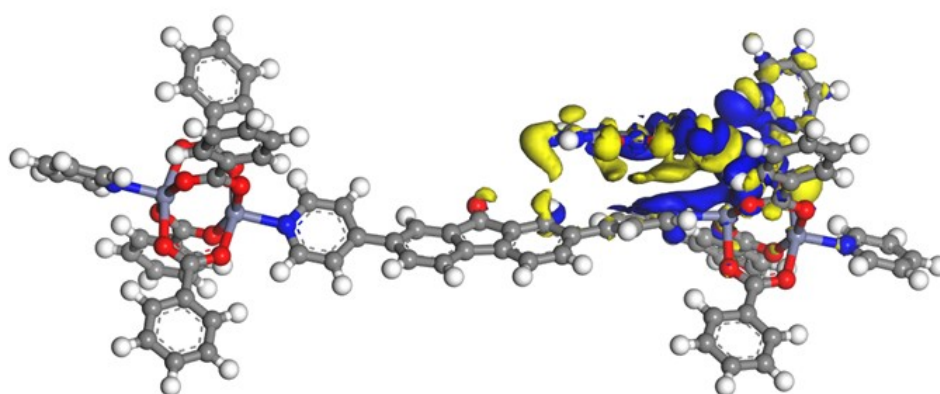
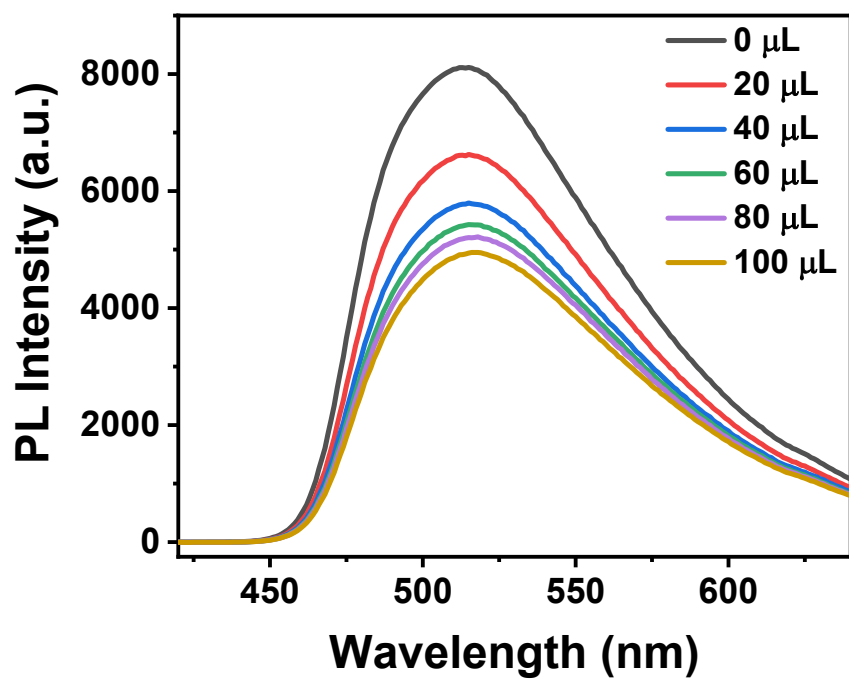**Figure S21.** Change in charge densities after ZnMOF-1 interacts with TriazFOX.

15

Figure S22. PL quenching spectra for 1 mg/ml ZnMOF-1 solutions in MeCN with additions of H_2O (20 μL addition each time).